4 Dark Matter Detection with XENON and DARWIN

Peter Barrow, Laura Baudis, Sandro D'Amato, Domenico Franco, Michelle Galloway, Andrea Gmuer, Shingo Kazama, Gaudenz Kessler, Alexander Kish, Andreas James, Daniel Mayani, Francesco Piastra, Yuehuan Wei, Julien Wulf

in collaboration with:
Albert Einstein Center for Fundamental Physics Bern, Columbia University, UCLA, UCSD, INFN, University of Münster, Coimbra University, Subatech, The Weizmann Institute of Science, University of Mainz, SJTU, MPIK Heidelberg, Stockholm University, Rice University, University of Chicago, University of Bologna, Nikhef and Amsterdam University, Purdue University, NYU of Abu Dhabi

(XENON Collaboration)

Dark matter reveals its presence on various astronomical scales, including our own galaxy, through its gravitational attraction. Its intrinsic nature is largely unknown, and existing data are compatible with models where the dark matter consists of new particles, which are not part of the Standard Model [1]. A compelling class of candidates are weakly interacting massive particles (WIMPs), which are predicted by various extensions to the Standard Model, such as supersymmetry or large extra dimensions. WIMPs must be stable, or very long-lived and are expected to have very weak couplings to ordinary matter [2]. Direct detection experiments are designed to look for scattering signatures of galactic WIMPs off atomic nuclei. The expected nuclear recoil energies are below a few tens of keV, and the rates are lower than $\sim$1 event per year and kg of target material [3].

While no direct evidence for WIMPs exists, the sensitivity of direct searches has seen a dramatic increase over the last decade, a development which was largely lead by the dual-phase, xenon time projection chamber (TPC) technique [3–5]. Large liquid xenon TPCs such as XENON100 [6, 7], LUX [8, 9] and PandaX [10] constrain the cross section of WIMPs on nucleons down to $\sim$few $\times 10^{-46}$ cm^2 regime, while the upcoming XENON1T [11] and the planned DARWIN detector [12, 13] are expected to improve upon these results by two and three orders of magnitude, respectively [14].

We are still operating the XENON100 experiment at the Laboratori Nazionali del Gran Sasso (LNGS) and are in the process of commissioning the XENON1T detector in the underground laboratory. In the following we will present the latest XENON100 results, and discuss the status of the XENON1T experiment. We will conclude by presenting a sensitivity study to WIMP dark matter for the next-generation DARWIN detector.

[1] G. Bertone, D. Hooper and J. Silk, Phys. Rept. **405** (2005) 279.

[2] M.W. Goodman and E. Witten, Phys. Rev. D31 (1985) 3059.

[3] Laura Baudis, J.Phys. G43 (2016) no.4, 044001.

[4] L. Baudis, Phys. Dark Univ. 1 (2012) 94.

[5] Laura Baudis, Annalen der Physik 528 (2016) 74-83.

[6] E. Aprile *et al.*, XENON Collaboration, Phys. Rev. Lett. 107 (2011) 131302.

[7] E. Aprile *et al.*, XENON100, Astropart. Phys. 35 (2012) 573.

[8] D. S. Akerib *et al.* [LUX Collaboration], Nucl. Instrum. Meth. A **704** (2013) 111.

[9] D. S. Akerib *et al.* [LUX Collaboration], Phys.Rev. D93 (2016) no.7, 072009.

[10] A. Tan *et al.* [PandaX Collaboration], "Dark Matter Search Results from the Commissioning Run of PandaX-II," arXiv:1602.06563 [hep-ex].

[11] E. Aprile *et al.*, XENON Collaboration, JCAP 1604 (2016) no.04, 027.

[12] L. Baudis, DARWIN Consortium, J.Phys.Conf.Ser. 375 (2012) 012028.

[13] Laura Baudis, PoS IDM2010 (2011) 122.

[14] M. Schumann, L. Baudis, L. Bütikofer, A. Kish and M. Selvi, JCAP **1510** (2015) no.10, 016.

4.1 Annual Modulation Search with XENON100

XENON100 is a 161 kg double-phase xenon TPC, which employs two arrays of low-radioactivity, VUV-sensitive photomultipliers (PMTs) to detect the prompt (S1) and proportional (S2) scintillation light signals induced by particles interacting in the target volume, containing 62 kg of ultra-pure liquid xenon (LXe). The remaining 99 kg of LXe act as an active veto shield against background radiation.

In 2012, over an integrated period of 225 live days, the experiment has reached its design sensitivity of 2×10^{-45} cm^2 at 55 GeV/c^2 and 90% confidence level on the spin-independent

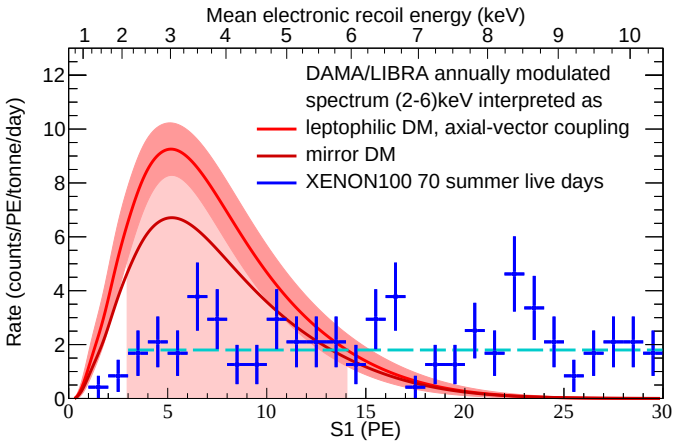

FIG. 4.1 – The DAMA/LIBRA modulated spectrum (red), interpreted as WIMPs scattering through axial-vector interactions, as it would be seen in the XENON100 detector. The 1σ band includes statistical and systematic uncertainties. The DAMA/LIBRA modulated spectrum interpreted as luminous dark matter is very similar, whereas the interpretation as mirror dark matter is indicated separately (dark red). The (blue) data points are XENON100 data from the 70 summer live days with their statistical uncertainty. The expected average XENON100 rate is also shown (dashed cyan). The shaded region from (3-14) PE was used to quantify the confidence level of exclusion. Figure from [18].

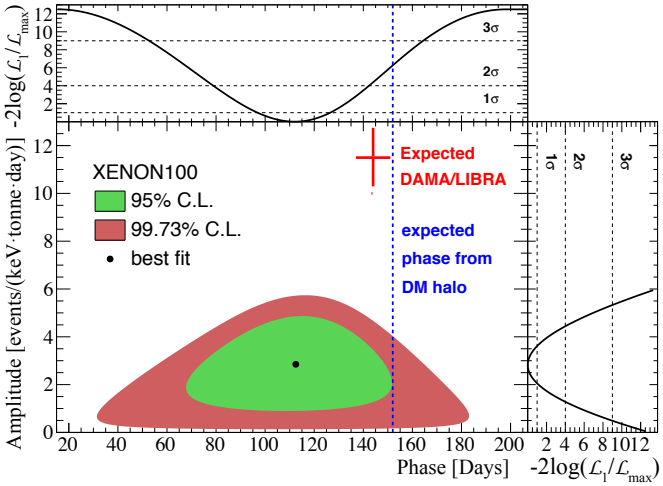

FIG. 4.2 – The XENON100 best-fit, 95% and 99.73% confidence level contours as a function of amplitude and phase relative to January 1, 2011 for period P = 1 year. The expected DAMA/LIBRA signal with statistical uncertainties only and the phase expected from a standard dark matter (DM) halo are overlaid for comparison. Top and side panels show -2log(Λ_1/Λ_{max}) as a function of phase and amplitude, respectively, along with two-sided significance levels. Figure from [19].

elastic WIMP-nucleon scattering cross section [15], and obtained the best limit at the time for spin-dependent interactions [16].

The same data have been used to search for axions and axion-like particles [17] and, most recently, to probe the DAMA/LIBRA modulation result, which is the only long-standing claim for a dark matter detection. Since DAMA/LIBRA has no discrimination power between nuclear recoils (NRs) and electronic recoils (ERs), a possibility to reconcile the observed signal with the null-results from other experiments consists in assuming a dark matter axial-vector coupling to electrons, in so-called *leptophilic models*. To test this hypothesis, we performed two analyses focused on the interaction between a potential dark matter candidate and electrons in the LXe. The first study used the overall electronic recoil rate and allowed to exclude leptophilic models as explanation for the DAMA/LIBRA signal [18]. Figure 4.1 shows the XENON100 ER rate, along with the expectations from DAMA/LIBRA in such models.

The second study exploited the periodic variations of the electronic recoil event rate in the 2 - 6 keV energy range [19]. The measured phase of 112±15 days (also observed for multiple-scatters, which are not WIMP candidates) disfavours the interpretation of a modulation due to a standard dark matter halo at $2.5\,\sigma$ confidence level, as shown in Fig. 4.2. In addition, the annual modulation interpreted as a dark matter signature with axial-vector coupling of dark matter particles to electrons was excluded at $4.8\,\sigma$ confidence level [19].

[15] E. Aprile *et al.*, XENON Collaboration, Phys. Rev. Lett. 109 (2012) 181301.

[16] E. Aprile *et al.*, XENON Collaboration, Phys. Rev. Lett. 111 (2013) 021301.

[17] E. Aprile *et al.*, XENON Collaboration, Phys. Rev. D 90 (2014) 062009.

[18] E. Aprile *et al.* XENON Collaboration, Science **349** (2015) no.6250, 851.

[19] E. Aprile *et al.* XENON Collaboration, Phys. Rev. Lett. 115 (2015) 091302.

4.2 Improving the Sensitivity with XENON1T

The XENON1T experiment is under commissioning in Hall B at LNGS (see Fig. 4.3). It uses a total of 3.3 t of LXe operated in a cryostat surrounded by a 9.6 m diameter and 10 m high water Cherenkov shield [20]. The cryostat is a double-walled super-insulated pressure vessel, made of stainless steel. The inner vessel houses the liquid xenon, the TPC and two PMT arrays. The TPC is made of interlocking PTFE panels, and the drift field homogeneity is achieved with equidistant copper field shaping rings connected with high-ohmic HV resistors. The photo-sensors are arranged in two arrays, containing 127 PMTs above the target in the gas phase, and 121 PMTs at the bottom, immersed in the liquid.

FIG. 4.3 – The XENON1T experiment in Hall B of LNGS. The water Cherenkov shield with a picture of the cryostat, its support structure and the pipe housing the cryogenic lines and cabling are seen on the left side. The infrastructure building, containing the LXe storage and purification systems, the krypton distillation column, the electronics and DAQ, as well as the cryogenic systems on the top level is seen on the right.

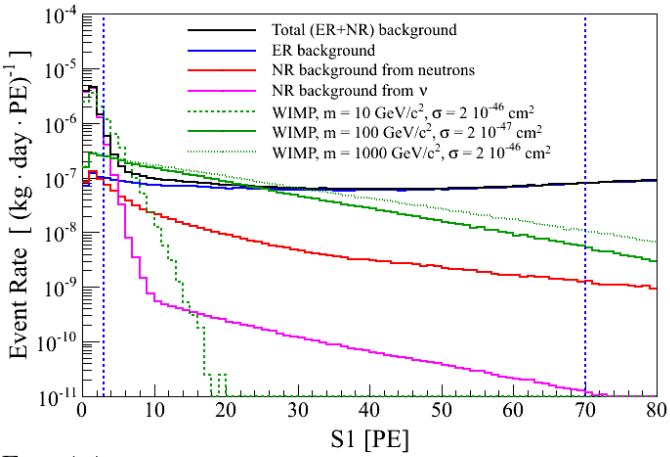

FIG. 4.4 – Predicted energy spectra for the total background and its components. The three examples for WIMP signals correspond to different masses and interaction cross sections at the limit of the XENON1T sensitivity. The vertical blue lines delimit the energy region (in the prompt scintillation signal, S1) used for the sensitivity calculation. Events with S2 $>$ 150 PE are selected, and an 99.75% ER rejection with 40% acceptance to NRs is assumed. Figure from [11].

At UZH, we contributed to the design, construction, tests and integration of the TPC, to the development and tests in liquid xenon of the photomultiplier tubes, to their readout electronics and light calibration system, to the signal and high-voltage cables and connectors, as well as to the radioassay of materials employed to construct the detector [21]. We are also involved in the background modeling and in simulating the electric drift field and the light collection efficiency of the TPC.

The performance of XENON1T and its sensitivity to WIMP interactions [11] were studied by Monte Carlo simulation. The radio-assays of all detector components were used for a realistic background model. The average rates of the various ER and NR backgrounds were calculated and their energy spectra are shown in Fig. 4.4, along with WIMP-induced signals. An inner fiducial region containing 1 t of LXe mass was considered here, as well as 99.75% ER rejection efficiency and a 40% acceptance for NRs.

The main contribution to the ER background originates in the decays of the ^{222}Rn daughters ($\sim$85%), assuming a 10 μBq radon level. Other sources of ER background are the radioactive isotope ^{85}Kr, present at the level of 2×10^{-11} in ^{nat}Kr ($\sim$4%), solar neutrinos scattering elastically off electrons in the medium ($\sim$5%), detector materials ($\sim$4%), and the double-beta decay of ^{136}Xe, which is present in natural Xe at 8.9% (1%) with a half-life of 2.17×10^{21} y.

The NR background is caused by radiogenic neutrons emitted by detector components (mostly in (α, n) reactions), by neutrons produced in interactions of cosmic muons with the rock, the concrete of the underground laboratory and the detector materials, and by coherent neutrino-nucleus scattering (CNNS) from ^{8}B neutrinos at low energies and atmospheric neutrinos at higher energies. The sensitivity to spin-independent WIMP-nucleon interactions after 2 t y exposure has a minimum cross section value of 1.6×10^{-47} cm^2, for a WIMP mass of 50 GeV/c^2 [11] which implies an improvement over XENON100 by two orders of magnitude.

[20] E. Aprile *et al.*, XENON Collaboration, JINST **9** (2014) 11006.

[21] E. Aprile *et al.*, XENON Collaboration, Eur. Phys. J. C **75** (2015) no.11, 546.

4.3 The XENON1T Time Projection Chamber

In October 2015 the assembly of the XENON1T TPC began at LNGS in an above-ground cleanroom. After methodical cleaning to remove impurities and etch away radioactive surface contamination the 74 copper field-shaping rings of the field cage were mounted on the cylindrical PTFE support structure which has a height and a diameter of $\approx$1 m. Reflector panels and fibre optic cables were installed. The fibres are used to uniformly distribute light inside the TPC for PMT calibration. Two sets of high voltage chains were installed as well, each consisting of 73 resistors (5 GΩ each) bridging neighbouring rings, allowing for an optimal electric field of 1 kV/cm. In parallel the top PMT array was installed inside the TPC diving bell.

Next, cathode, anode and gate electrodes were mounted which provide a radially-uniform electric field across the TPC. They consist of wires or hexagonal meshes stretched across

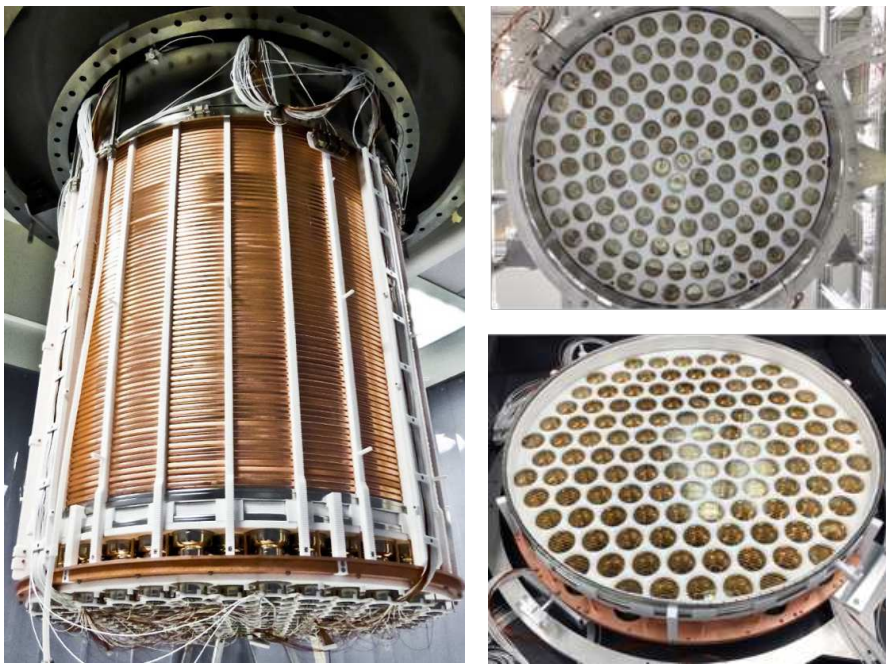

FIG. 4.5 –
Left: the XENON1T TPC during its installation in the underground cleanroom at LNGS. The PTFE pillars and the Cu field shaping rings are clearly visible, as well as the bottom PMT array and the dome of the inner cryostat. Right: the top and bottom photodetector arrays. These detector 'eyes' contain 127 and 121 3-inch, Hamamatsu R11410-21 PMTs, respectively.

stainless steel rings (grids). The bottom screening mesh, cathode, and small PTFE reflectors were installed directly onto the bottom PMT array. The gate grid was gently lifted and affixed onto the top TPC ring, followed by the anode grid, with 5 mm insulating spacers in between the two grids. The xenon liquid/gas interface will reside between these two electrodes. Then the small PTFE reflector panels were assembled and the protective mesh for the PMTs was placed on top. Level meters that measure by capacitance the height of the liquid xenon were installed onto the top TPC ring. The bottom PMT array was mounted to the field cage, and monitoring devices such as temperature sensors and diagnostic PMTs were installed. Finally, the TPC was wrapped and secured to prepare for transport to the underground laboratory.

On November 4th the TPC was transported into Hall B and wheeled inside the water tank for installation. Using a set of 3 winches from the top dome of the water tank, the delicate instrument, now close to 500 kg, was slowly and carefully raised from the bottom of the tank, through a hole in the cleanroom floor, and up to the dome of the tank. Figure 4.5 shows the TPC mounted to the dome inside the underground water tank. At this point, the integration of the TPC with other XENON1T subsystems, such as the DAQ and cryogenics systems, began. The high voltage feed-through, piping for liquid xenon, and cabling for PMTs, fibre optics, sensors, and electrodes were connected. After many visual and mechanical checks, electrical tests, and a final cleaning, the stainless steel vessel that contains the liquid xenon was lifted and sealed to enclose the TPC. The installation of the XENON1T detector was a success, and the instrument is currently under commissioning.

[22] G. Angloher *et al.*, CRESST Collaboration, Eur.Phys.J. C74 (2014) 3184.

[23] R. Agnese *et al.*, SuperCDMS Collaboration, *Search for Low-Mass WIMPs with SuperCDMS* (2014) arXiv:1402.7137.

[24] M. Xiao *et al.*, PandaX Collaboration, Sci. China Phys. Mech. Astron. **57** (2014) 2024.

[25] M. Bossa, DarkSide Collaboration, JINST 9 (2014) C01034.

[26] D.S. Akerib *et al.*, LUX Collaboration, (2013) arXiv:1310.8214.

[27] M.G. Boulay, DEAP Collaboration, J.Phys.Conf.Ser. 375 (2012) 012027.

[28] E. Aprile, XENON Collaboration, Springer Proc. Phys. **148** (2013) 93.

[29] D.C. Malling *et al.*, *After LUX: The LZ Program*, (2011) arXiv:1110.0103.

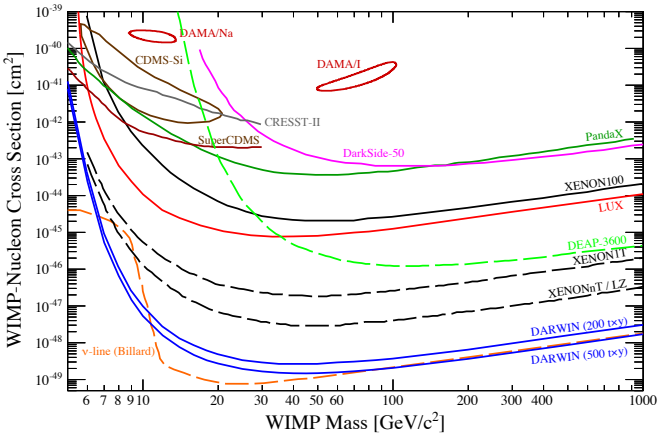

FIG. 4.6 –
Spin-independent WIMP-nucleon scattering results: Existing upper limits from the CRESST-II [22], SuperCDMS [23], PandaX [24], DarkSide-50 [25], XENON100 [15], and LUX [26] experiments, along with projections for DEAP3600 [27], XENON1T [28], XENONnT [20], LZ [29], and DARWIN [12] are shown. DARWIN is designed to probe the entire parameter region for WIMP masses above $\sim$6 GeV/c^2, until the neutrino background (ν-line) will start to dominate the recoil spectrum. Figure adapted from [14].

4.4 The XENONnT and DARWIN projects

After the commissioning of the XENON1T detector, our efforts are focused on data analysis and on a new TPC design for the planned 7 t XENONnT upgrade for which we are testing new, improved photosensors. Many major components in XENON1T have been designed such that they can be reused in XENONnT, such as the water Cherenkov shield, the xenon storage vessel, the cryogenic and purification systems, the cryostat support, the outer cryostat vessel and the connection pipe to the building. The DAQ system for XENON1T can be upgraded for the $\sim$200 extra channels of XENONnT without new developments. The main challenge is to build a new, larger TPC and to further lower the intrinsic backgrounds from radon and krypton.

DARWIN is an ultimate, xenon-based WIMP detector with a sensitivity goal down to $\sim 10^{-49}$ cm^2. At these cross-sections, neutrino interactions, which cannot be reduced by target fiducialization, will limit the sensitivity to WIMP scatters [12]. With a total LXe mass of 50 t, this project would be the successor of XENONnT, and installed in the same Hall B at LNGS (possibly in a larger Cherenkov shield). Our R&D is focused on the design and prototyping of the time projection chamber, on Monte Carlo simulations of the radioactive background, on new light read-out schemes and tests of light sensors in noble liquids, material screening with high-purity germanium spectroscopy, as well as on the science impact of the facility. Recently we have performed a detail study of the sensitivity of the DARWIN instrument to spin-independent and spin-dependent WIMP-nucleon scattering interactions. Taking into account realistic backgrounds from the detector itself as well as from neutrinos, we examined the impact of exposure, energy threshold, background rejection efficiency and energy resolution on the dark matter sensitivity. With an exposure of 200 t y and assuming detector parameters which have been already demonstrated experimentally, spin-independent cross sections as low as 2.5×10^{-49} cm^2 can be indeed probed, as shown in Fig. 4.6. Additional improvements in terms of background rejection and exposure will further increase the sensitivity, while the ultimate WIMP science reach will be limited by neutrinos scattering coherently off the xenon nuclei [14].

We additionally perform charge and light yield measurements of nuclear and electronic recoils in LXe at low energies, which are necessary to define accurate energy scales in noble liquid dark matter detectors. To this end, we have built a new, small TPC (Xurich-II), that we are currently operating in the neutron beam at the D-D fusion generator at the Physik-Institut. Our goal is to measure the NR versus ER discrimination as a function of drift field, and to determine the charge and light yield of low-energy nuclear recoils.